QUBIC - The Q & U Bolometric Interferometer for Cosmology
QUBIC - The Q & U Bolometric Interferometer for Cosmology

S.A. Torchinsky[1], ***Peter Ade***[6], ***Giorgio Amico***[7], ***Didier Auguste***[8], ***Jonathan Aumont***[7], ***Stefano Banfi***[7], ***Gustavo Barbaràn***[7], ***Paola Battaglia***[7], ***Elia Battistelli***[7,23], ***Alessandro Baù***[7], ***Benoit Bélier***[7], ***David G. Bennett***[7], ***Laurent Bergé***[8], ***Jean Philippe Bernard***[7], ***Marco Bersanelli***[7], ***Marie Anne Bigot Sazy***[1], ***Nathat Bleurvacq***[1], ***Juan Bonaparte***[7], ***Julien Bonis***[7], ***Emory F. Bunn***[7], ***David Burke***[5], ***Daniele Buzi***[7], ***Alessandro Buzzelli***[7], ***Francesco Cavaliere***[7], ***Pierre Chanial***[1], ***Claude Chapron***[1], ***Romain Charlassier***[1], ***Fabio Columbro***[7], ***Gabriele Coppi***[7], ***Alessandro Coppolecchia***[7,23], ***Giuseppe D'Alessandro***[7,23], ***Paolo De Bernardis***[7,23], ***Giancarlo De Gasperis***[7], ***Michele De Leo***[7], ***Marco De Petris***[7], ***Andres Di Donato***[7], ***Louis Dumoulin***[7], ***Alberto Etchegoyen***[13], ***Adrián Fasciszewski***[13], ***Cristian Franceschet***[9], ***Martin Miguel Gamboa Lerena***[14], ***Beatriz Garcia***[13], ***Xavier Garrido***[8], ***Michel Gaspard***[8], ***Amanda Gault***[19], ***Donnacha Gayer***[5], ***Massimo Gervasi***[4], ***Martin Giard***[10], ***Yannick Giraud Héraud***[1], ***Mariano Gómez Berisso***[7], ***Manuel González***[2], ***Marcin Gradziel***[7], ***Laurent Grandsire***[1], ***Eric Guerard***[7], ***Diego Harari***[7], ***Vic Haynes***[7], ***Sophie Henrot Versillé***[8], ***Duc Thuong Hoang***[1], ***Federico Incardona***[7], ***Eric Jules***[8], ***Jean Christophe Hamilton***[1], ***Nicolas Holtzer***[13], ***Jean Kaplan***[1], ***Andrei Korotkov***[7], ***Christian Kristukat***[2], ***Luca Lamagna***[7,23], ***Soutiris Loucatos***[1], ***Thibaut Louis***[8], ***Raùl Horacio Luterstein***[13], ***Bruno Maffei***[22], ***Stefanos Marnieros***[21], ***Silvia Masi***[7,23], ***Angelo Mattei***[7], ***Andrew May***[3], ***Mark McCulloch***[3], ***Maria C. Medina***[8], ***Lorenzo Mele***[7], ***Simon J. Melhuish***[3], ***Aniello Mennella***[4], ***Ludovic Montier***[21], ***Louise Mousset***[1], ***Luis Mariano Mundo***[12], ***James Murphy***[5], ***John Anthony Murphy***[5], ***Emiliano Olivieri***[21], ***Creidhe O'Sullivan***[5], ***Alessandro Paiella***[7,23], ***Francois Pajot***[10], ***Andrea Passerini***[4], ***Hernan Pastoriza***[2], ***Alessandro Pelosi***[7], ***Camille Perbost***[1], ***Maurizio Perciballi***[7], ***Federico Pezzotta***[7], ***Francesco Piacentini***[7,23], ***Michel Piat***[1], ***Lucio Piccirillo***[3], ***Giampaolo Pisano***[6], ***Gianluca Polenta***[7], ***Damien Prêle***[1], ***Roberto Puddu***[7], ***Damien Rambaud***[10], ***Pablo Ringegni***[12], ***Gustavo E. Romero***[16], ***Maria Salatino***[1,24], ***Alessandro Schillaci***[7], ***Claudia G. Scóccola***[14], ***Stephen P. Scully***[5], ***Sebastiano Spinelli***[4], ***Guillaume Stankowiak***[1], ***Michail Stolpovskiy***[1], ***Federico Suarez***[15], ***Andrea Tartari***[1,23], ***Jean Pierre Thermeau***[1], ***Peter Timbie***[19], ***Maurizio Tomasi***[9], ***Mathieu Tristram***[8], ***Gregory S. Tucker***[17], ***Carole E. Tucker***[6], ***Sylvain Vanneste***[8], ***Daniele Viganò***[9], ***Nicola Vittorio***[20], ***Fabrice Voisin***[1], ***Robert Watson***[3], ***Francois Wicek***[8], ***Mario Zannoni*** [4], ***and Antonio Zullo***[7]

[1] *Astroparticle Physics & Cosmology, Observatoire de Paris, CNRS/IN2P3, Université Paris-Diderot, CEA, France*
[2] *Centro Atómico Bariloche and Instituto Balseiro, Argentina*
[3] *University of Manchester, UK*
[4] *Universita di Milano-Bicocca, Italy*
[5] *Maynooth University, Ireland*
[6] *Cardiff University, UK*
[7] *Universita La Sapienza, Roma, Italy*
[8] *Laboratoire de l'AccélIrateur Linéaire, (CNRS/IN2P3), France*
[9] *Universita degli studi di Milano, Italy*
[10] *Institut de Recherche en Astrophysique et Planétologie, Toulouse, France*
[11] *Centro Atómico Constituyentes, Argentina*
[12] *Grupo de Ensayos Mecànicos Aplicados, Argentina*
[13] *Comision Nacional de Energia Atomica, Argentina*
[14] *Facultad de Ciencias Astronómicas y Geofísicas, Argentina*
[15] *Instituto de Tecnologías en Detección y Astropartículas, Argentina*
[16] *Instituto Argentino de Radioastronomía, Argentina*
[17] *Brown University, USA*
[18] *Richmond University, USA*
[19] *University of Wisconsin, USA*
[20] *Università di Roma Tor Vergata, Italy*
[21] *Centre de Sciences Nucléaires et de Sciences de la Matière, CNRS, Paris, France*
[22] *Institut d'Astrophysique Spatiale, Paris, France*
[23] *Istituto Nazionale di Fisica Nucleare, Italy*
[24] *Kavli Institute for Particle Astrophysics and Cosmology, Stanford University, USA*

Keywords: Cosmology, Gravitational Waves, Inflation, Interferometry, self-calibration, aperture synthesis
Mots-clefs: Cosmologie, Ondes gravitationnelles, interérométrie, auto-étalonnage, synthèse d'ouverture

Abstract:

QUBIC is a millimetre wave telescope to measure the polarization B-modes in the Cosmic Microwave Background (CMB). Primordial B-modes polarization has yet to be detected, but it is are expected to be visible in the CMB as a result of Inflation in the fraction of a second after the Big Bang during which primordial gravitational waves are produced. The detection of B-modes in the CMB is fundamental to our understanding of the Universe and will help confirm the Standard Model of Cosmology, including Inflation. QUBIC uses a novel technique of bolometric interferometry, merging together the techniques of optical interferometry, in which the interference pattern is imaged on a detector array, and the radio interferometry technique of aperture synthesis, making a powerful wide band instrument capable of the radio technique of self calibration. This technique also permits QUBIC to use the frequency dependence of the synthesized beam to do spectral imaging of the CMB. As a result, QUBIC has a unique capability to reduce systematic and foreground effects from the measurement. QUBIC is currently integrated, and undergoing test at the facility at APC. A description of the instrument and characterization results will be presented.

Résumé:
QUBIC est un télescope d'ondes millimétriques pour mesurer le mode B de la polarisation du Fond Diffus Cosmologique (CMB). Jusqu'à présent, ce signal n'a pas été détecté, mais il est attendu d'après la théorie standard de la cosmologie qui prévoit une période d'inflation de l'Univers pendant la première fraction de seconde de son histoire. C'est à cette époque que des ondes gravitationnelles primordiales sont générées et qui doivent légèrement polariser le Fond Diffus en mode tensoriel. QUBIC est donc une expérience fondamentale pour notre connaissance de l'Univers et de la physique. QUBIC exploite une toute nouvelle technique d'observation, l'interférométrie bolométrique. On mélange la technique d'interférométrie optique qui crée une image d'interférogramme sur la matrice de détecteurs, et la technique radio de synthèse d'ouverture. La combinaison produit un instrument très puissant pour le filtrage des signaux non désirables venant de l'instrument et de l'avant plan en utilisant les techniques de l'imagerie spectrale et d'auto-étalonnage. QUBIC est actuellement en cours d'intégration dans le laboratoire APC et les tests de caractérisation sont en cours. Une description de l'instrument et de ses performances sera présentée.

1 Introduction

QUBIC is an experiment based on an idea proposed by Ali et al. [1, 2] for a millimetre wave bolometric interferometer. It is designed to measure the B-mode polarization anisotropies of the Cosmic Microwave Background (CMB). The QUBIC design combines the sensitivity of Transition Edge Sensors (TES), bolometric detectors with the systematic effects and foreground control provided by its interferometric design.
The control of astrophysical foregrounds, in particular, is a factor of increasing importance in CMB polarization experiments, and QUBIC allows us to disentangle sub-bands in each main frequency band thanks to its spectral imaging capability, which is deeply rooted in the interferometric nature of the instrument.
QUBIC will operate from the ground observing the sky in two main spectral bands centered at 150 and 220 GHz [3] and will be deployed in Argentina, at the Alto Chorrillos site. The team is currently finalizing the laboratory tests of the technical demonstrator, a simplified version of the instrument that will be installed at the site during 2019 and will demonstrate the technical and scientific potential of our approach. The final instrument will be deployed during 2020.

2 The Instrument

Figure 1 shows a schematic of QUBIC. The signal from the sky enters the cryostat through a High-Density Polyethylene (HDPE) window. Then, a rotating half-wave plate modulates the polarization, and a polarizing grid selects one of the two linear polarization components. An array of 400 back-to-back corrugated horns collects the radiation and re-images it onto a dual-mirror optical combiner that focuses the signal onto two orthogonal TES detector arrays. A dichroic filter placed between the optical combiner and the focal planes selects the two frequency bands, centred at 150 GHz and 220 GHz. The right panel of Figure 1 shows a 3D rendering of the inner part of the cryostat. A key part of the instrument is an array of movable shutters placed between the primary and secondary feed-horn arrays. Each shutter acts as an RF switch (a blade that can slide into a smooth circular waveguide), which is used to exclude particular baselines when the instrument operates in calibrating mode. This permits the exploitation of the calibration strategy called "self-calibration", which is a key feature of the QUBIC systematic effects control. A detailed description of the instrument is found in [4] and the theory of self-calibration for QUBIC is described in [5].

3 Measurement, Self-Calibration, and Spectral Imaging

3.1 Signal Model and Synthetic Beam

In QUBIC, the optical combiner focuses the radiation emitted by the secondary horns onto the two focal planes so that the image that forms on the detector arrays is the result of the interference arising from the sum of the

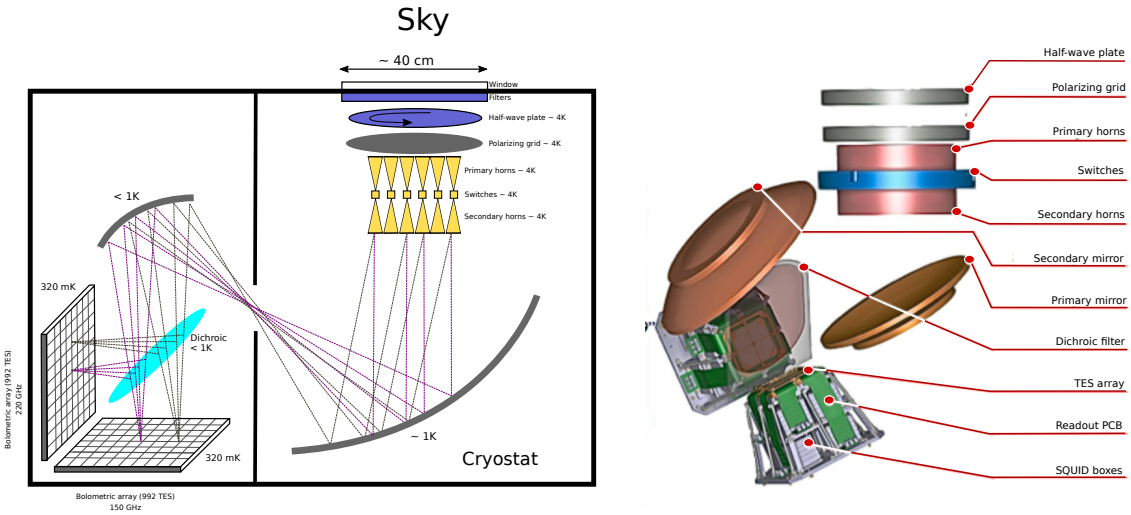

Figure 1 – (Left) Schematic of the **QUBIC** *instrument. The window aperture is about 40 cm; the cryostat is about 1.41 m in diameter and 1.51 m in height; (right) 3D rendering of the inner part of the cryostat. TES, Transition Edge Sensor.*

fields radiated from each of the 400 apertures.
Therefore, the signal measured at time t by a detector p on the focal plane is:

$$R(p,\nu,t) = K\left[S_I(p,\nu) + \cos(4\,\phi_{\rm HWP}(t))\,S_Q(p,\nu) + \sin(4\,\phi_{\rm HWP}(t))\,S_U(p,\nu)\right], \quad (1)$$

where ν is the frequency, $\phi_{\rm HWP}$ is the angle of the half-wave plate at time t, and K is an overall calibration constant that takes into account the efficiency of the optical chain. The three terms $S_{I,Q,U}$ in Equation (1) represent the sky signal in intensity and polarization convolved with the so-called synthetic beam.
Figure 2 shows the simulation of QUBIC observing a point source in the far field with all 400 antennas open to the sky. The image formed on each of the focal planes (right panel of Figure 2) is an interference pattern formed by peaks and lobes. This equivalent to the "dirty-image" produced in radio aperture synthesis (see for example [6]).
Therefore, if X is the signal from the sky (either in intensity, I, or polarization, Q, U), then the measured signal on the pixel p is $S_X(p) = \int X(\mathbf{n}) B^p_{\rm synth}(\mathbf{n}) d\mathbf{n}$. This means that QUBIC data can be analyzed similarly to the data obtained from a normal imager, provided that we build a window function of the synthetic pattern for each pixel.

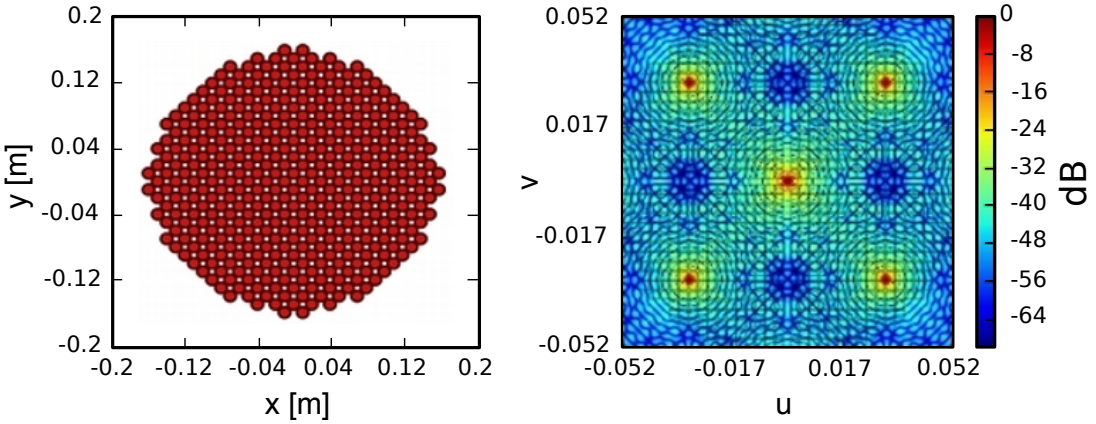

Figure 2 – (Left) QUBIC aperture plane showing all 400 antennas open to the sky; (right) the interference pattern formed on each of the focal planes when the instrument is observing a point source located in the far field vertically along the instrument line-of-sight. The u and v coordinates are defined as: $u = \sin\theta\cos\phi$ and $v = \sin\theta\sin\phi$, where θ and ϕ are the angles on the celestial sphere defining the synthetic beam.

3.2 Self-Calibration

QUBIC self-calibration is a technique derived from the technique in radio-interferometry. This technique evolved from the original idea in the 1970's of "phase-closure" [7, 8, 9] to become in the early 1980's "self-calibration" [10,

11]. In QUBIC, self-calibration exploits the redundant interferometric patterns obtained when we selectively close various combinations of the 400 apertures.
To understand the basic concept, see the four panels of Figure 3. The top-right plot shows the interference pattern arising from a horn configuration in which only two horns are open and all the others are closed (top-left). The panels in the bottom row show that if we open any other horn pair with the same baseline, we should ideally obtain exactly the same interference pattern. Furthermore, Bigot-Sazy et al. [5] showed that the configuration in which only two horns are open is equivalent to the complementary arrangement in which only two horns are closed.
We can now use the fact that, for an ideal instrument, the interferometric pattern depends only on the baseline. This allows us to characterize the instrumental parameters and non-idealities using an observation mode called self-calibration. In the self-calibration mode, pairs of horns are successively shut while QUBIC observes an artificial partially-polarized source (a microwave synthesizer or a Gunn oscillator) in the far field. Then, we reconstruct the signal measured by each individual pair of horns in the array and compare them.
The point now is that if the source is stable and carefully monitored, then redundant baselines correspond to the same mode of the observed field, so that a different signal between them can only be due to photon noise or instrumental systematic effects. Using a detailed parametric model of the instrument, we can fully recover the instrument parameters through a non-linear inversion process. The updated model of the instrument can then be used to reconstruct the synthetic beam and improve the map-making, reducing the leakage from E- to B-modes.
In Figure 4 (adapted from [5]), we show the improvement in the power spectrum estimation with self-calibration according to three schemes. Even with 1 s per baseline (corresponding to a full day dedicated to self-calibration), we can reduce significantly the $E \rightarrow B$ leakage. This leakage can be further reduced by spending more time in self-calibration. The three B-mode power spectra in black solid lines are the theoretically-expected spectra for three values of the parameter r, i.e., the ratio between the amplitudes of the tensor and scalar fluctuations during inflation.

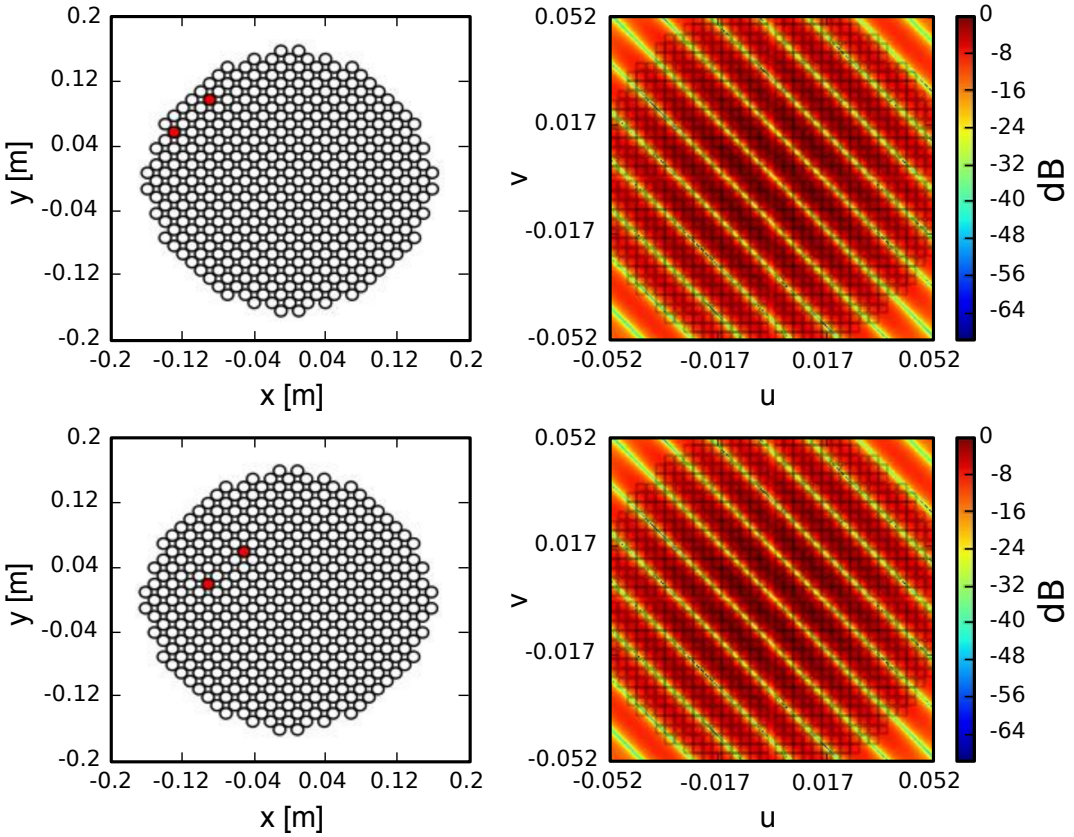

Figure 3 – Schematic of QUBIC self-calibration. The pictures in the two rows show that if we open any pair of horns with a given baseline, then in absence of systematic effects, we should measure exactly the same interference pattern.

3.3 Spectral Imaging

The interferometric nature of QUBIC provides us with another unique feature: the possibility to split the data of each main frequency band into sub-bands, thus considerably increasing the leverage in the control of astrophysical foregrounds.

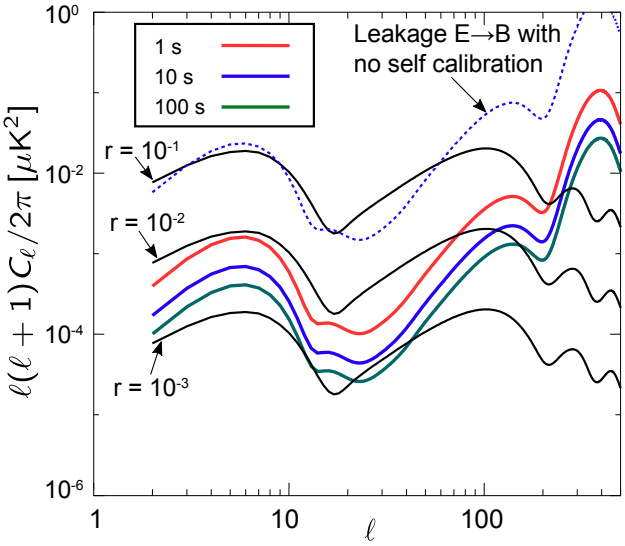

Figure 4 – Improvement in the recovery of the B-mode power spectrum as a function of the time spent in the self-calibration mode. The three curves drawn with black solid lines represent theoretical B-mode power spectra calculated for three different values of the tensor-to-scalar ratio, r. (adapted from [5])

This feature is called "spectral imaging", and its concept is explained schematically in Figure 5. The left panel of Figure 5 shows the synthetic beams (solid lines) and main feedhorn beams (dashed lines) at two monochromatic frequencies. The figure clearly shows that the sidelobe peaks are well separated, and this sensitivity of the synthetic beam to the frequency can be exploited to separate the various sub-bands in the input data.

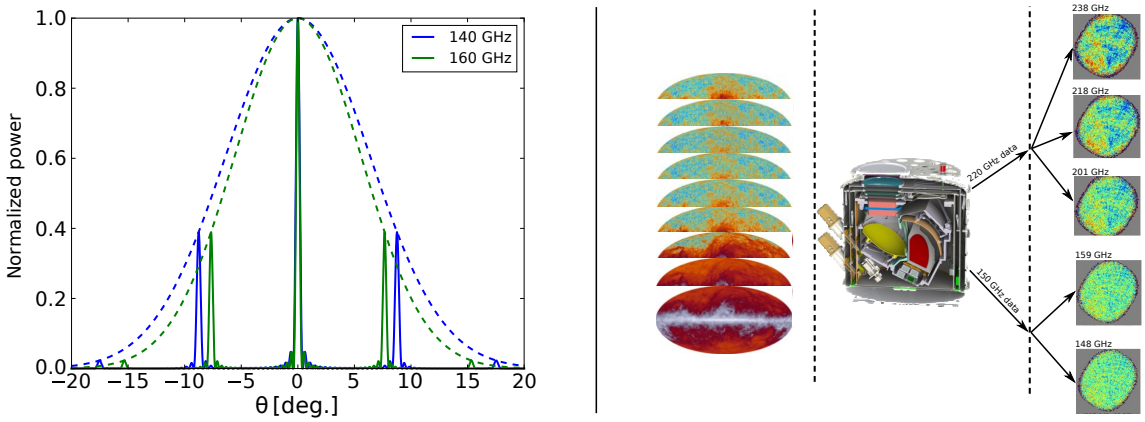

Figure 5 – (Left) Cut of the synthesized beam for two monochromatic signals. The main central peaks superimpose each other, but the first lobes are separated so that they can be resolved. The dashed lines represent the horn beams. (Right) Schematics representing the ability to resolve spectral sub-bands in each of the main QUBIC bands. The instrument first separates the wide-band sky signal into two main bands (150 and 220 GHz), then we further separate each band into sub-bands thanks to the spectral sensitivity of the synthesized beams. The Planck maps shown on the left have the only purpose of explaining the concept.

The right panel of Figure 5 shows schematically the process of sub-band separation in the data analysis. The instrument measures the wide-band sky signal and splits the two main frequency bands of 150 GHz and 220 GHz. Then, the main bands are further separated in the data analysis pipeline by exploiting the frequency sensitivity of the synthetic beam.
As spectral imaging opens new possibilities of foreground control, it also requires component separation codes that have been not been developed yet. We are currently working on a first detailed assessment of its potential and will soon submit a specific paper on spectral imaging.

4 The QUBIC Site

QUBIC will be deployed in Argentina, at the Alto Chorrillos mountain site (24°11′11.7″ S; 66°28′40.8″ W, altitude of 4869 m a.s.l.) near San Antonio de los Cobres, in the Salta province [12] (see the left panel of

Figure 6). The zenith optical depth measured at 210 GHz, τ_{210}, is <0.1 for 50% of the year and <0.2 for 85% of the year. Winds are usually mild (<6 m/s for 50% of the year), which suggests limited turbulence.
While the statistics for τ_{210} in Alto Chorrillos is worse than that of an Antarctic site (either South Pole or Dome C), the site access and logistics are easier. Our trade off is also justified by the following two facts: (i) the atmospheric emission is not polarized to first order, and (ii) a bolometric interferometer intrinsically rejects large-scale atmospheric gradients, which produce most of the atmospheric noise.
The right panel in Figure 6 (adapted from [4]) shows the overall site quality. In the plot, we see the uncertainty in the tensor-to-scalar ratio, r, as a function of the fraction of usable time for two years of operations. The circled point shows the estimate for the case in which zero or 12 h a day are spent in calibration mode. The plot shows that for a 30% usable time (a conservative estimate for our site), we can reach a sensitivity on r of 10^{-2} with two years of operations.

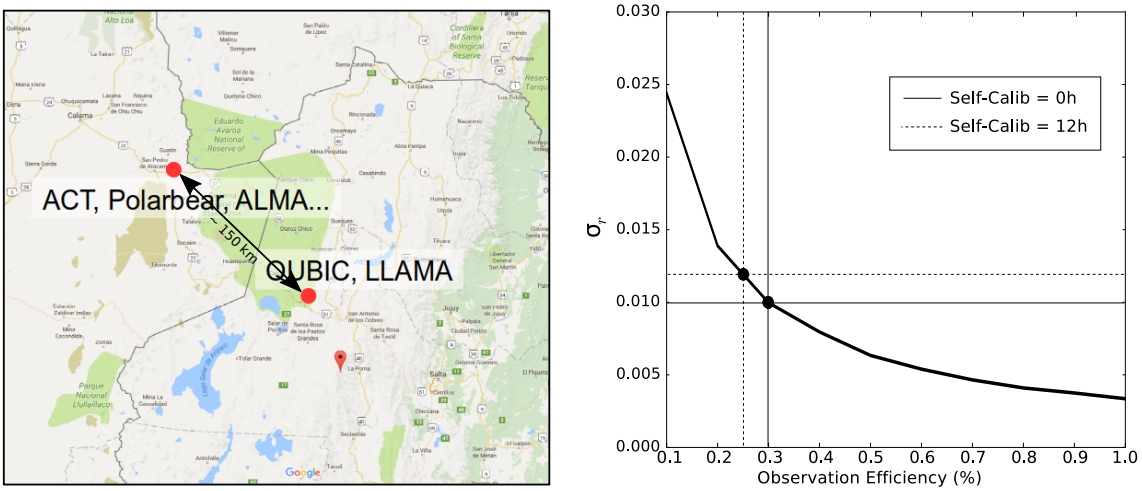

Figure 6 – (Left) Location of the QUBIC site compared to the Atacama plateau; (right) uncertainty in the tensor-to-scalar ratio, r, as a function of the fraction of usable time for two years of operations. The parameter r was computed considering noise-only simulations.

5 Current Status

QUBIC is currently in the phase of laboratory calibration of the so-called "Technological Demonstrator" (TD). The TD has a reduced focal plane and horn array with respect to the full instrument. In particular, the TD has only one-quarter of the 150-GHz TES focal plane, an array of 8×8 horns and switches, and a smaller optical combiner. The TD will demonstrate the feasibility of the bolometric interferometry both in the laboratory and in the field.
Figure 7 shows various QUBIC components. Panel (a) shows one of the two cryogenic detection chains. On top of the chain, one can see the TES focal plane. Panel (b) shows the array of the 8×8 back-to-back dual-band corrugated horns interfaced with the switch array. Panels (c) and (d) show the 1 K box before and during the integration into the QUBIC cryostat.
Figure 8 shows the setup in the laboratory at Astroparticle Physics and Cosmology (APC) in Paris. The calibration source reflects into the QUBIC cryostat window from a flat mirror. At a distance of over 11 m, the calibration source is well within t he far-field of QUBIC. The calibration source is a strong source easily detected by the detector array as seen in Figure 9. QUBIC was scanned in azimuth, and the beam mapped by one of the pixels is shown in Figure 10.
QUBIC TD is currently being calibrated at the Astroparticle Physics and Cosmology laboratory in Paris (APC). The testing phase will continue through Spring/Summer 2019 after which QUBIC will be shipped to Argentina and installed at the site for a first-light test foreseen within 2019. Components for the final instrument are being manufactured and tested in Europe, including the 20×20 horn array and switches, upgraded mirrors, and the two full TES detector arrays of 1024 detectors for each of the frequency bands (150 GHz and 220 GHz). The dual band QUBIC with complete detector arrays is expected to be operational on the Alto Chorrillos site in 2020.

6 Conclusions

QUBIC is a new way to measure the polarization of the CMB. It combines the sensitivity of TES bolometric arrays with the control of systematic effects that are typical of interferometers. This is a key asset in CMB

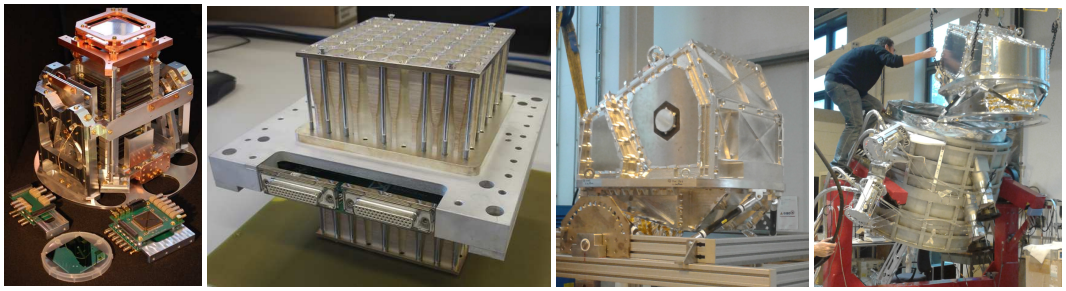

*Figure 7 – Status of the current QUBIC development. (**a**) The cryogenic section of the QUBIC detection chain; (**b**) the 8 × 8 back-to-back horns and switches array employed in the Technological Demonstrator (TD); (**c**) the integrated 1 K box; (**d**) integration of the 1K box in the cryostat shell.*

Figure 8 – (left) Photo of QUBIC in the foreground and the calibration source mounted on the wall at the far end of the room during the laser alignment procedure. (right) Photo of QUBIC looking along the line-of-sight from the calibration source. The reflection of the window is clearly visible in the flat mirror.

polarization experiments where high sensitivity must be combined with similarly low levels together with a high level of control of systematic and foreground effects. QUBIC responds to this challenge with the key features of self-calibration and spectral imaging, which are possible thanks to the interferometric nature of the instrument. A technological demonstrator is currently being tested in the laboratory and will soon be deployed in Argentina for a first-light test. We forecast the installation of the final instrument and the start of scientific operations during 2020, opening the way for a new generation of instruments in the field of Cosmic Microwave Background polarimetry.

QUBIC is funded by the following agencies. France: ANR (Agence Nationale de la Recherche) 2012 and 2014, DIM-ACAV (Domaine d'Interet Majeur—Astronomie et Conditions d'Apparition de la Vie), CNRS/IN2P3, CNRS/INSU. Italy: CNR-Programma Nazionale Ricerche in Antartide until 2016, Istituto Nazionale di Fisica Nucleare since 2017. Argentina: Secretaría de Gobierno de Ciencia, Tecnología e Innovación Productiva, Comisión Nacional de Energía Atómica, Consejo Nacional de Investigaciones Científicas y Técnicas. U.K.: the University of Manchester team acknowledges the support of STFCgrant ST/L000768/1. Ireland: James Murphy and David Burke acknowledge postgraduate scholarships from the Irish Research Council. Duc Hoang Thuong acknowledges the Vietnamese government for funding his scholarship at APC. Andrew May acknowledges the support of an STFCPhD Studentship.

7 References

[1] Ali, S.; Rossinot, P.; Piccirillo, L.; Gear, W. K.; Mauskopf, P.; Ade, P.; Haynes, V.; Timbie, P., MBI: Millimetre-wave bolometric interferometer, American Institute of Physics Conference Series, **2002** Vol 616, pp. 126-128, doi:10.1063/1.1475615

[2] Tucker, G.S. et al. New Astronomy Reviews 47 (2003) 11731176

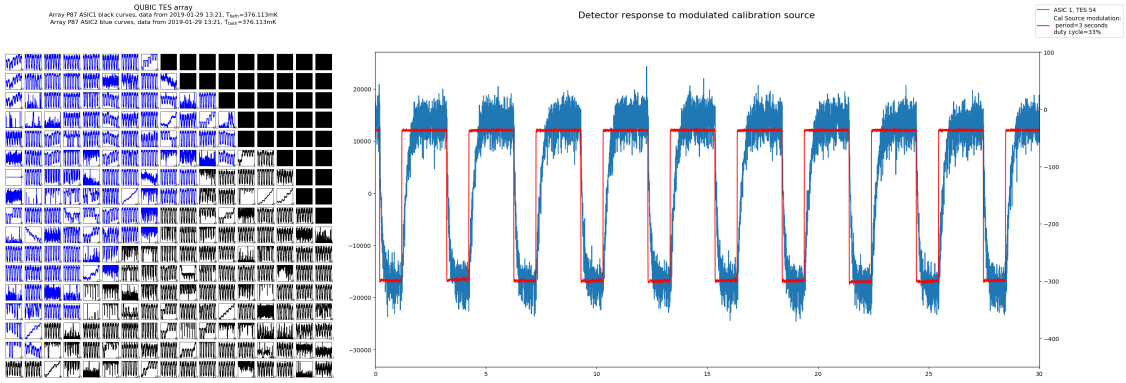

Figure 9 – Left: Detection of the modulated calibration source by the QUBIC detector array. The array shown here is for the Technological Demonstrator instrument and it covers one quarter of the full focal plane. Right: Comparison of the source modulation (red) with the detected signal (blue) for one of the TES detectors

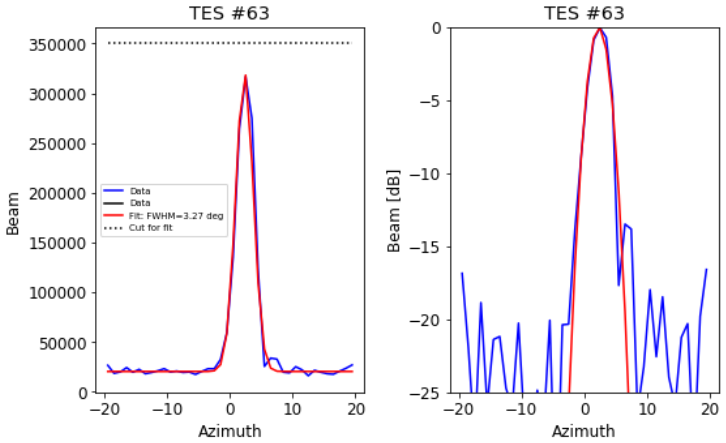

Figure 10 – An azimuth scan of the calibration source is shown here for one pixel. On the left, in linear intensity, and on the right on a dB scale.

[3] Tartari, A.; Aumont, J.; Banfi, S.; Battaglia, P.; Battistelli, E.S.; Baù, A.; Bélier, B.; Bennett, D.; Bergé, L.; Bernard, J.P.; et al. QUBIC: A Fizeau Interferometer Targeting Primordial B-Modes. *J. Low Temp. Phys.* **2015**, *181*, doi:10.1007/s10909-015-1398-3.

[4] Aumont, J.; Banfi, S.; Battaglia, P.; Battistelli, E.S.; Baù, A.; Bélier, B.; Bennett, D.; Bergé, L.; Bernard, J.P.; Bersanelli, M.; et al. QUBIC Technical Design Report. *arXiv* **2016**, arXiv:1609.04372.

[5] Bigot-Sazy, M.A.; Charlassier, R.; Hamilton, J.; Kaplan, J.; Zahariade, G. Self-calibration: An efficient method to control systematic effects in bolometric interferometry. *Astron. Astrophys.* **2013**, *550*, A59, doi:10.1051/0004-6361/201220429.

[6] Thompson, A. R.; Moran, J. M.; Swenson, Jr., G. W., Interferometry and Synthesis in Radio Astronomy, 3rd Edition, **2017**, doi:10.1007/978-3-319-44431-4

[7] Hogbom 1974, A&AS, 15, 417

[8] Fort & Yee 1976, A&A 50, 19

[9] Readhead & Wilkinson 1978, ApJ, 223, 25

[10] Cornwell & Wilkinson, 1981 MNRAS, 196, 1067

[11] Pearson, T. J., & Readhead, A. C. S. 1984, ARA&A, 22, 97

[12] De Bernardis, P.; Ade, P.; Amico, G.; Auguste, D.; Aumont, J.; Banfi, S.; Barbarán, G.; Battaglia, P.; Battistelli, E.; Baù, A.; et al. QUBIC: Measuring CMB polarization from Argentina. *Bol. Asoc. Argent. Astron. Plata Argent.* **2018**, *60*, 107–114.